Research Article

Broadband photon squeezing control using microring embedded gold grating for LiFi-quantum link

J. Ali[1] · P. Youplao[2] · K. Chaiwong[3] · I. S. Amiri[4] · S. Punthawanunt[5] · N. Pornsuwancharoen[6,7] · P. Yupapin[6,7]

Abstract
A broadband wavelength photon squeezing system using a Panda-ring resonator embedded a gold grating is proposed. The selected laser source is input into the system via an input port, from which the nonlinear Kerr effect induced by the two nonlinear side rings and coupled into the center ring. Besides, the wavelength scattering is affected by the gold grating and the photon output wavelengths. By adjusting the suitable two side ring radii, where there is four type squeezing photons obtained. The obtained wavelengths are ranged from 1.30 to 170 μm with the center wavelength of 1.55 μm, where the maximum input power is 50 mW. From which the optimum spectrum range (FSR) of 22 nm is achieved. In applications, the up and downlink LiFi transmission can be formed using the whispering gallery mode node, in which the squeezed photons and the add port output can be used to form the communication. The signal modulation and demodulation can be applied via the device add and other ports, while the cable transmission is also available via the through the port connection. By using the TiO_2 reflector, the transmitted photons at the add port can also be controlled an attenuated, which can be used for single photon source and communication.

Keywords Squeezed photons · Quantum source · LiFi-quantum link · Quantum communication

1 Introduction

Squeezed light within the micro (nano) devices based on the current fabrication technologies have become the promising method for practical applications [1–4]. The main advantage is that quantum computing device and system scale will be reduced and suitable for the realistic application, where such features such as low power consumption, random squeezing state and secured data remain and useful for quantum code(decode) usages. Recently, Ali et al. [5] have shown that the squeezed coherent light (photon) within the conventional microring resonator can be categorized to be 4 types, in which the key effect was the coupling control of the two side rings. The squeezed light beams are obtained when the uncertainty value ($\Delta E \cdot \Delta t$) is saturated [6]. Light fidelity (LiFi) network has become the promising technique for modern network technology [7–9], where the advantage over the wire (cable) network due to the more transmitted data capacity than the wire (cable) network. Besides, the quantum information platform can be easily implemented [10, 11]. In this article, we have proposed the photon squeezing system, in which the electric field is input and circulated within the system described by $\boldsymbol{E_Z} = E_0 \boldsymbol{e}^{-i\boldsymbol{k}_z \boldsymbol{Z} - \omega \boldsymbol{t}}$, E_0 is the initial electric field amplitude

✉ N. Pornsuwancharoen, nithiroth.pornsuwancharoen@tdtu.edu.vn; ✉ P. Yupapin, preecha.yupapin@tdtu.edu.vn | [1]Laser Centre, IBNU SINA ISIR, Universiti Teknologi Malaysia, 81310 Johor Bahru, Malaysia. [2]Department of Electrical Engineering, Faculty of Industry and Technology, Rajamangala University of Technology Isan, Sakon Nakhon Campus, 199 Phungkon, Sakon Nakhon 47160, Thailand. [3]Department of Electrical and Electronics Engineering, Faculty of Industrial Technology, Loei Rajabhat University, Loei 42000, Thailand. [4]Division of Materials Science and Engineering, Boston University, Boston, MA 02215, USA. [5]Multidisciplinary Research Laboratory, Faculty of Science and Technology, Kasem Bundit University, Bangkok 10250, Thailand. [6]Computational Optics Research Group, Advanced Institute of Materials Science, Ton Duc Thang University, District 7, Ho Chi Minh City, Vietnam. [7]Faculty of Applied Sciences, Ton Duc Thang University, District 7, Ho Chi Minh City, Vietnam.

SN Applied Sciences (2019) 1:482 | https://doi.org/10.1007/s42452-019-0487-3

Received: 20 January 2019 / Accepted: 12 April 2019

Published online: 22 April 2019

[12], where $\boldsymbol{E}_0$ is the electric field amplitude, $\boldsymbol{k_z} = \frac{2\pi}{\lambda}$ is the wave number in the direction of propagation (z-axis) and $\boldsymbol{\omega}$ is the angular frequency, where $\omega = 2\pi\gamma$ is the angular frequency, γ is the linear frequency. The wave-particle duality functions are ψ and ψ^*, where ψ^* is the complex conjugate of ψ. The new form of the time-dependent wave function is $\psi = A\boldsymbol{e}^{-i\frac{E_n}{\hbar}t}$, where $A = \boldsymbol{E}_0\boldsymbol{e}^{-ik_z}$. The particle (photon) energy is $E_n = nh\gamma$, *where* $n = 1, 2, 3, \ldots$ and h is the Plank's constant. Regarding the de Broglie–Bohm theory [13], where the wave function defines the evolution over time of the configuration by a guiding function, which is given by the Schrodinger equation. The squeezing state condition is the saturation of $\Delta E \cdot \Delta t = \hbar$, which affects the photon wave function being vanished. It means that the photon energy is squeezed and released from the system, from which the system stability remains. In a simulation, four types of photon squeezing results are manipulated and plotted, from which the possible application of the system for LiFi-quantum link can be applied. The photon squeezing control can be managed by adjusting the two side ring radii, the reflector lengths within the system and varying the input power. The necessary background of the system is given. By using the graphical approach called the Optiwave program, the suitable parameters with the expected results are obtained. The verified the obtained results, the method known as the Matlab program is applied. In the manipulation, the practical parameters of the microring fabrication radius of 1.0 micron and others are confirmed [14].

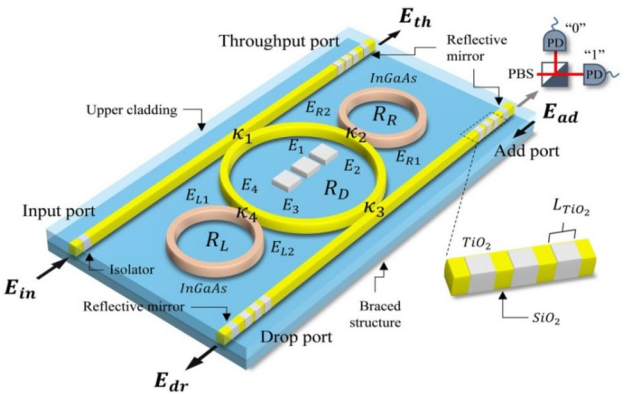

Fig. 1 A system model for broadband photon squeezing generation, where $\boldsymbol{E_{in}}$, $\boldsymbol{E_{th}}$, $\boldsymbol{E_{dr}}$, $\boldsymbol{E_{ad}}$ representing the fields for input, throughput, drop and add ports respectively. $\boldsymbol{R_R}$, $\boldsymbol{R_L}$, and $\boldsymbol{R_D}$ representing the radii for right, left, and the center rings respectively. All coupling coefficients, $\kappa_s = 0.5$. $\boldsymbol{R_D} = \boldsymbol{R_{Si}}$ silicon ring radius, *PBS* polarizing beam-splitter, *PD* photo-detector. The parameter of the ring $R_{Si} = 1.80$ µm, R_R and R_L are 1.20 µm, the reflectors (TiO_2) are 0.2–0.5 µm, the gold grating dimensions are $0.1 \times 0.1 \times 0.2$ µm, and the grating pitch is 50 nm. The InGaAs refractive index (n_0) is 2.9, the nonlinear refractive index (n_2) is 1.02×10^{-17} m^2 W^{-1} [16, 17], while n_{SiO_2} is 1.439 [18]. The waveguide loss is 0.5 dB mm^{-1}

2 Background

From Fig. 1, the monochromatic light source is input into the system, with the center wavelength is at 1.55 µm. The selected input power is fed into the microring resonator system, from which the partial light power is coupled into the input port and a system. The propagation waves are circulated within the system and degraded due to some losses. However, this is the successive operation, in which the nonlinear effect can be induced into the system, wherein some ways the self-pumping can be introduced and the short and high peak power obtained. Finally, the uncertainty will randomly reach the product of $\Delta E \cdot \Delta t$. In this case, the squeezed light (photon) is generated and used for LiFi up-down link node. The electric fields (E_s) within the system and device can formulate by the following equations [15].

$$\boldsymbol{E}_1 = \left(\sqrt{1-\gamma_1}\right)\left(\boldsymbol{j}\sqrt{\kappa_1}\boldsymbol{E_{in}} + \sqrt{1-\kappa_1}\boldsymbol{E}_4\boldsymbol{e}^{-\frac{\alpha}{2}\frac{L_d}{4} - \boldsymbol{jk_n}\frac{L_d}{4}}\right) - \boldsymbol{E}_1^* \tag{1}$$

$$\boldsymbol{E}_2 = \left(\sqrt{1-\gamma_2}\right)\left(\sqrt{1-\kappa_2}\boldsymbol{E}_1\boldsymbol{e}^{-\frac{\alpha}{2}\frac{L_d}{4} - \boldsymbol{jk_n}\frac{L_d}{4}} + \boldsymbol{j}\sqrt{\kappa_2}\boldsymbol{E_{R2}}\boldsymbol{e}^{-\frac{\alpha}{2}\frac{L_r}{2} - \boldsymbol{jk_n}\frac{L_r}{2}}\right) - \boldsymbol{E}_2^* \tag{2}$$

$$\boldsymbol{E}_3 = \left(\sqrt{1-\gamma_3}\right)\left(\sqrt{1-\kappa_3}\boldsymbol{E}_2\boldsymbol{e}^{-\frac{\alpha}{2}\frac{L_d}{4} - \boldsymbol{jk_n}\frac{L_d}{4}} + \boldsymbol{j}\sqrt{\kappa_3}\boldsymbol{E_{ad}}\right) - \boldsymbol{E}_3^* \tag{3}$$

$$\boldsymbol{E}_4 = \left(\sqrt{1-\gamma_4}\right)\left(\sqrt{1-\kappa_4}\boldsymbol{E}_3\boldsymbol{e}^{-\frac{\alpha}{2}\frac{L_d}{4} - \boldsymbol{jk_n}\frac{L_d}{4}} + \boldsymbol{j}\sqrt{\kappa_4}\boldsymbol{E_{L2}}\boldsymbol{e}^{-\frac{\alpha}{2}\frac{L_l}{2} - \boldsymbol{jk_n}\frac{L_l}{2}}\right) - \boldsymbol{E}_4^* \tag{4}$$

$$\boldsymbol{E_{th}} = \left(\sqrt{1-\gamma_1}\right)\left(\sqrt{1-\kappa_1}\boldsymbol{E_{in}} + \boldsymbol{j}\sqrt{\kappa_1}\boldsymbol{E}_4\boldsymbol{e}^{-\frac{\alpha}{2}\frac{L_d}{4} - \boldsymbol{jk_n}\frac{L_d}{4}}\right) - \boldsymbol{E}_{th}^* \tag{5}$$

$$\boldsymbol{E_{dr}} = \left(\sqrt{1-\gamma_3}\right)\left(\sqrt{1-\kappa_3}\boldsymbol{E}_{ad}^* + \boldsymbol{j}\sqrt{\kappa_3}\boldsymbol{E}_2\boldsymbol{e}^{-\frac{\alpha}{2}\frac{L_d}{4} - \boldsymbol{jk_n}\frac{L_d}{4}}\right) - \boldsymbol{E}_{dr}^* \tag{6}$$

$$\boldsymbol{E_{ad}} = \left(\sqrt{1-\gamma_3}\right)\left(\sqrt{1-\kappa_3}\boldsymbol{E_{dr}^*} + \boldsymbol{j}\sqrt{\kappa_3}\boldsymbol{E_3}\boldsymbol{e}^{-\frac{\alpha}{2}\frac{L_d}{4}-\boldsymbol{jk_n}\frac{L_d}{4}}\right) \tag{7}$$

Where $E_{th}^*, E_{dr}^*, E_{ad}^*, E_1^*, E_2^*, E_3^*, and E_4^*$ are the reflected optical fields of the reflectors, which can be formulated by following Eqs. (8)–(11). From the Eqs. (1)–(7), the electrical fields are given by $E_{ad}^* = nE_{ad}, E_{th}^* = nE_{th}, and E_{dr}^* = nE_{dr}$, where n is reflective percentage(ratio).

$$\boldsymbol{E_4^*} = \left(\sqrt{1-\gamma_1}\right)\left(\boldsymbol{j}\sqrt{\kappa_1}\boldsymbol{E_{ad}^*} + \sqrt{1-\kappa_1}\boldsymbol{E_1^*}\boldsymbol{e}^{-\frac{\alpha}{2}\frac{L_d}{4}-\boldsymbol{jk_n}\frac{L_d}{4}}\right) \tag{8}$$

$$\boldsymbol{E_3^*} = \left(\sqrt{1-\gamma_4}\right)\left(\sqrt{1-\kappa_4}\boldsymbol{E_4^*}\boldsymbol{e}^{-\frac{\alpha}{2}\frac{L_d}{4}-\boldsymbol{jk_n}\frac{L_d}{4}} + \boldsymbol{j}\sqrt{\kappa_4}\boldsymbol{E_{L1}^*}\boldsymbol{e}^{-\frac{\alpha}{2}\frac{L_l}{2}-\boldsymbol{jk_n}\frac{L_l}{2}}\right) \tag{9}$$

$$\boldsymbol{E_2^*} = \left(\sqrt{1-\gamma_3}\right)\left(\sqrt{1-\kappa_3}\boldsymbol{E_3^*}\boldsymbol{e}^{-\frac{\alpha}{2}\frac{L_d}{4}-\boldsymbol{jk_n}\frac{L_d}{4}} + \boldsymbol{j}\sqrt{\kappa_3}\boldsymbol{E_{dr}^*}\right) \tag{10}$$

$$\boldsymbol{E_1^*} = \left(\sqrt{1-\gamma_2}\right)\left(\sqrt{1-\kappa_2}\boldsymbol{E_2^*}\boldsymbol{e}^{-\frac{\alpha}{2}\frac{L_d}{4}-\boldsymbol{jk_n}\frac{L_d}{4}} + \boldsymbol{j}\sqrt{\kappa_2}\boldsymbol{E_{R1}^*}\boldsymbol{e}^{-\frac{\alpha}{2}\frac{L_r}{2}-\boldsymbol{jk_n}\frac{L_r}{2}}\right) \tag{11}$$

where n is the reflection ratio, E_{Add} is the electric field output from the add port, E_{dr} and E_{th} are the electric fields at the drop and throughput (through) ports in the system, respectively. The intensity insertion loss coefficients of the 3 dB couplers are γ_{is}, and κ_{is} are the coupling constants, α is the attenuation loss of light in the waveguide and $k_n = (2\pi/\lambda)n_{eff}$. L_d is the circumference of the center ring.

3 Simulation results

Regarding the successive filtering process of the system as shown in Fig. 1, when the peak amplitude of the center ring photons is at the resonance with the side rings, the amplitude squeezing photon occurs within the center ring of those rings. It only a single peak generates within the individual ring, in which the two ring radii are the same ($R_R = R_L < R_{Rmax}$), where R_{rmax} is the initial two side ring radii. For the phase squeezing photons, the higher squeezed photon powers than the amplitude ones occurs because the pumping photon powers obtained from the two side rings induced by the nonlinear Kerr effect are at the resonant conditions. There are two cases of the phase squeezing photons, which are (1) $R_R < R_L$) and $R_R > R_L$). Next, the quadrature squeezing photons can occur within the system with the various peaks, where the same conditions of the phase squeezing are applied but in these cases the various peaks are squeezed within the system. The photon number squeezing can occur when the two side ring radii $R_R = R_L > R_{Rmax}$.

However, the optimum photon cases are not easy to generate, from which the mixed among the squeezed types such as amplitude-phase, phase-quadrature and photon number-quadrature etc. are acceptable. In a calculation, the reflection of the electrical fields at the reflector (TiO_2) and gold grating can be given by the phase terms. Here, $E_{ad}^* = nE_{ad}, E_{th}^* = nE_{th}, and E_{dr}^* = nE_{dr}$, where n is the reflection ratio. The drop port output field of the successive filter is the required signal. The involved phenomena of this system is the nonlinear Kerr effect that can give the system having the high power output, and the Bragg wavelength can give the light scattering and the broadening output. In addition, there is effect of the reflected power introduced into the system from the TiO_2 at the device portends, where the suitable reflector lengths will be selected. The Kerr effect is given by the refractive index equation, which is ultimately reflected in the refractive index, given by the relationship as $n = n_0 + n_2 I = n_0 + n_2 P/A_{eff}$, where n_0 and n_2 are the linear and nonlinear refractive indices, respectively. I is the optical intensity and P is the optical power, where A_{eff} is the effective mode core area of the device. For the microring resonator, the effective mode core areas range from 0.1 to 0.5 μm^2 [14]. The Bragg wavelength is given by $\lambda_B = 2\, n_e \bigwedge$, where n_e is the effective refractive index of the grating in the waveguide, and is the grating period. By using the graphical approached program called the Optiwave, the selected parameters were applied and given in the related figure captions. The input laser wavelength of 1.55 micron with the peak power of 25 and 50 mW was used for simulation, which can obtain the suitable power for LiFi link. The high power laser can get a more nonlinear effect that can induce the broadband photon output. The reflected material is applied by embedded on the microring resonator portend. The optical isolated is also applied at the input port, which can protect the feedback into the input source. In practice, the output power at the add port can be reduced by adjusting the reflected material (TiO_2) [18], which can provide the required squeezed photons, for an instant, a single photon output. In this case, the squeezed photons can be obtained by adjusting the suitable reflector length and the two side ring radii, which there are four types of squeezing states, which are (1) amplitude squeezing, (2) phase squeezing, (3) quadrature squeezing and (4) photon number squeezing. The number of photons with different wavelengths can provide broadband photon source applications. Moreover, the electronic and plasmonic inputs (outputs) are also available by connecting to the gold and stacked layers of silicon–graphene–gold to the applied devices [19].

The reflector (TiO_2) dimensions are wide × length × dept h = 0.1 μm × 0.1 μm × 0.3 μm. The gold grating dimensions are 0.1 × 0.1 × 0.3 μm, and the grating pitch is 60 nm. The

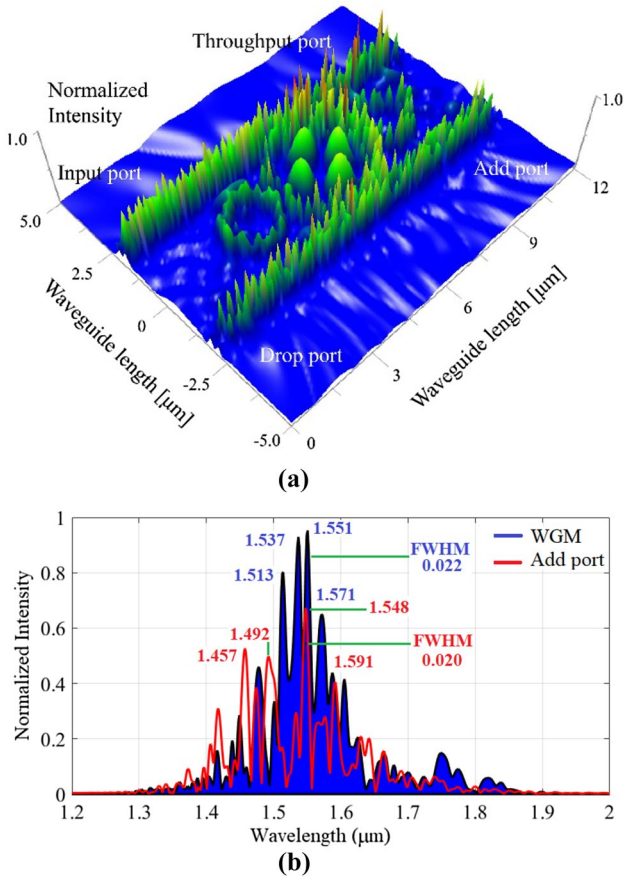

Fig. 2 Results of the amplitude squeezing state, where $R_R = 720$ nm, $R_L = 720$ nm, $R_D = 1.55$ μm, the input power is 25 mW, FWHM is ~ 20 –22 nm, where **a** the Optiwave and **b** the Matlab results

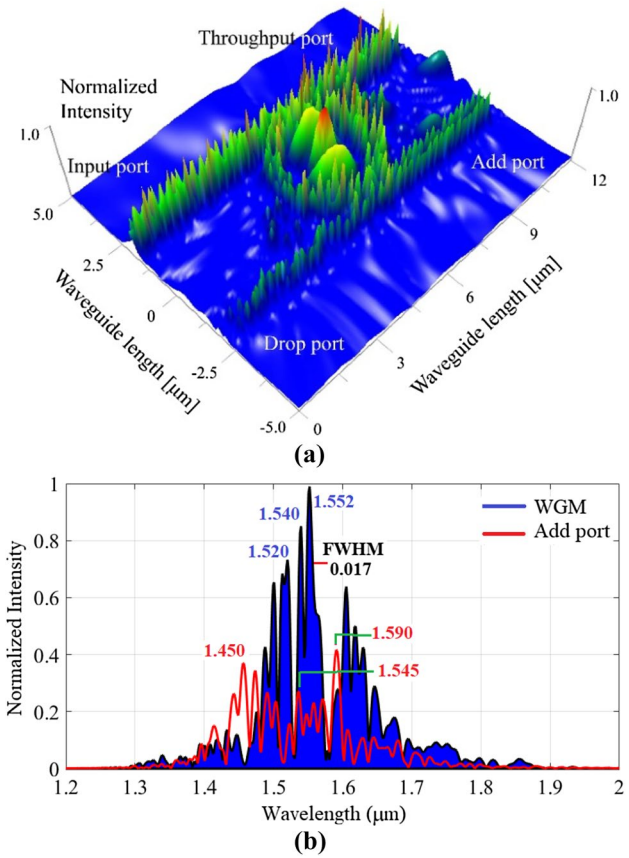

Fig. 3 Results of the phase squeezing state, where $R_R = 620$ nm, $R_L = 500$ nm, $R_D = 1.55$ μm, the input power is 25 mW, FWHM is ~ 17 nm, where **a** the Optiwave and **b** the Matlab results

used waveguide loss is 0.10 dB mm^{-1}, and the core effective area is 0.30 μm^2. The results of the squeezed photons with different types are plotted as shown in Figs. 2, 3, 4, 5, 6. The four types of the squeezing photons are plotted in Figs. 2, 3, 4, 5, where the output spectrum of the output power, free spectrum ranges (FSRs) and the spectral widths ($\Delta\lambda$) are also plotted. The parameters of the different ring radii are given in the related figure captions. The multi-wavelength photons are also plotted in Fig. 6. Figure 2 shows the result of the amplitude squeezing. The coupling effect is introduced to the two side rings by the center ring, while the coupling effect is introduced to the centering by the phase modulators, where (a) the squeezed photons within the system, (b) the broad spectrum of the photons within the system and add port. The free spectral range is 17 nm. The full width at half maximum is ~ 20 – 22 nm. Similarly, the other types of the squeezing photons are obtained and shown in Figs. 3, 4, 5. The broadband wavelength photons are plotted in Fig. 6, where there are two different input powers plotted, where the higher input power gives the broader wavelength spectrum output. It is due to the nonlinear Kerr effect induced by the two side rings and coupled into the center ring. However, in practice, the suitable input power can be desired. The advantages of the proposed system are (1) the squeezing photon control can offer the required photon broadening and power. From which the reflector length (TiO_2) can be suitably selected to obtain the required photon output at the WGM and add port, which can be used for single photon form and communication. The entangled photon output can also be arranged and used for quantum cryptography by adding the polarization components at the add port output. Moreover, the use of the quantum sensors based-on photons and single photon are also possible. Moreover, the squeezing state is randomly generated whenever the uncertainty product is saturated with $\Delta E \Delta t = \hbar$, which is the benefit of quantum aspect for secure information.

This is the small scale device that can be embedded within the modern application such as a mobile phone. The used parameters are the practical sizes that can be fabricated, wherein the references are already given. The simulation was simulated with the 20,000 round-trip times, from which the simulation was obtained. However, the

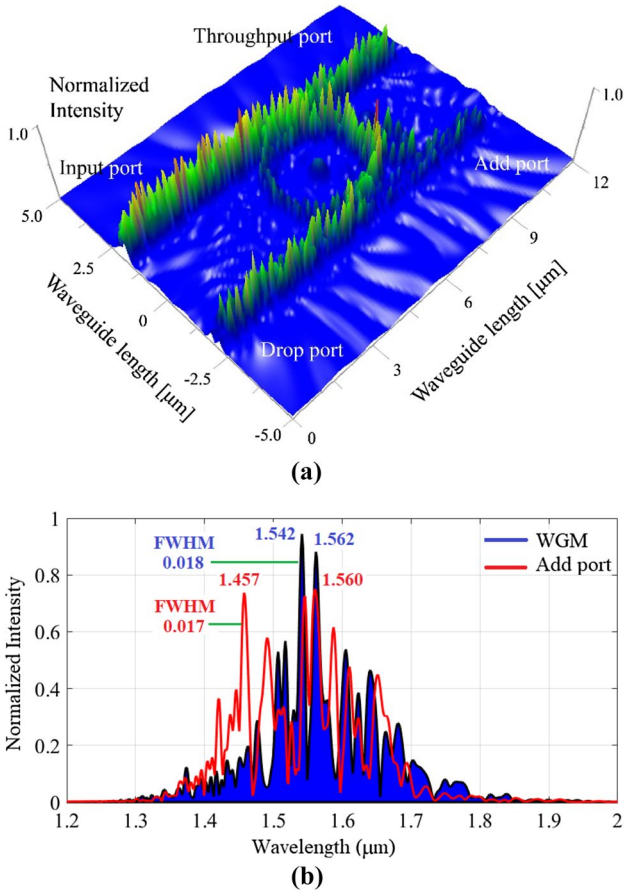

Fig. 4 Result of the quadrature squeezing state, where $R_R = 620$ nm, $R_L = 590$ nm, $R_D = 1.55$ μm, the input power is 25 mW, FWHM is ~17–18 nm, where **a** the Optiwave and **b** the Matlab results. In this case, the squeezing is occurred out of the center ring. However, it may some errors occur

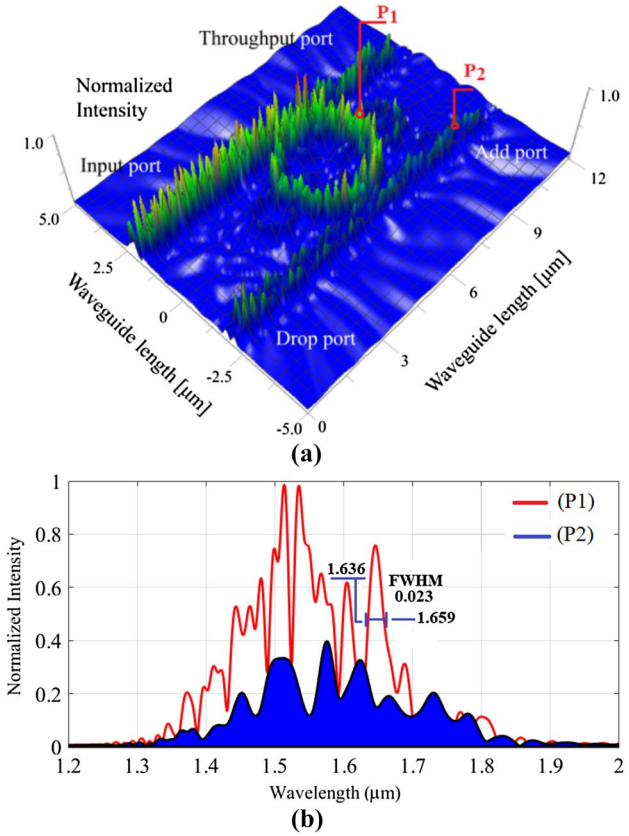

Fig. 5 Shows the result of the photon number squeezing state, where $R_R = 620$ nm, $R_L = 520$ nm, $R_D = 1.50$ μm, the input power is 25 mW, FWHM is 22 nm, where **a** the Optiwave and **b** the Matlab results. In this case, the squeezing is occurred on the ring circumference

output signals are the quantum codes (bits) that they are the random outcomes, which mean that the repeatability is not required.

4 Conclusion

We have demonstrated that the squeezing of light within the microring system embedded a gold grating can offer the broadband photon source, which has shown the promising results for broad applications. After some successive round trips of the input optical fields, the resonant squeezed photons are generated by the induced nonlinear effect and the uncertainty saturation condition. By using the graphical approach called the Optiwave program, the suitable parameters with the expected results are obtained, from which the verified method known as the Matlab program was applied. In the manipulation, the practical parameters of the microring fabrication radius of 500 nm and others are confirmed [14]. The general forms of the obtained should be seen as following: (1) the single peak in the center ring, with low power, where $R_R = R_L$, (2) a single peak or few peaks in the center and side rings, with high peak power when $R_R > R_L$ or $R_R < R_L$, (3) several peaks or many peaks outside the center ring, with medium high peak power, where $R_R \neq R_L$, (4) many peaks outside on the center ring circumference, with medium high peak power, where $R_R = R_L >$ radius side ring. The required add pot output is the low attenuated power for quantum communication. However, there may be some source errors occur that lead to have the little bit different from the ideal system. Generally, the various forms of the input signals can be an electrical signal, optical signal or magnetic spin, which can be applied via the stacked layers of the silicon–graphene–gold materials [20]. The obtained wavelength band is ranged from 1.30 to 1.80 μm, which suitable for various

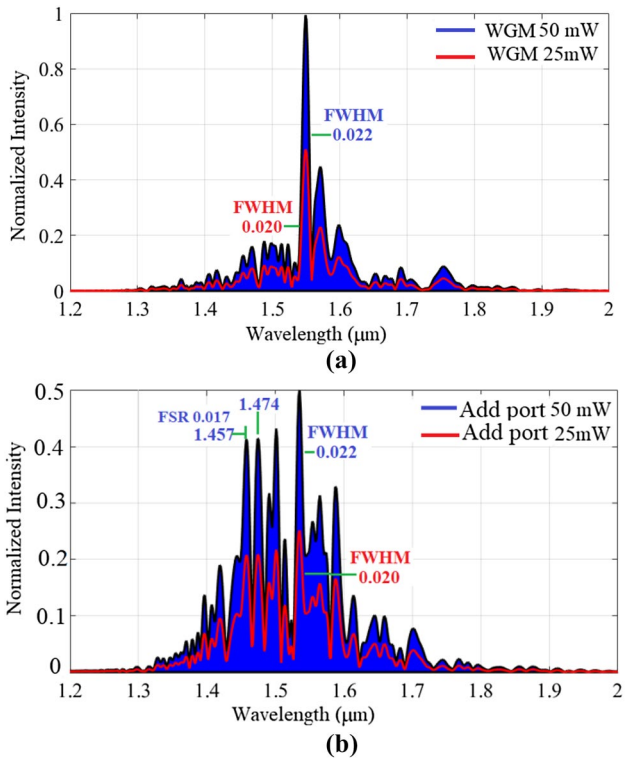

Fig. 6 The broadband photon results obtained at the WGM (**a**) and add port (**b**) with the two different input powers of 25 and 50 mW, where **a** R_R = 620 nm, R_L = 520 nm, R_D = 1.50 μm, the input is 25 mW, the input power is 25 mW, FWHM is ~20–22 nm, **b** R_R = 620 nm, R_L = 520 nm, R_D = 1.50 μm, the input is 25 mW, FWHM is ~20–22 nm and FSR is 17 nm. The optimum broadening wavelength range is from ~1.30–1.7 μm. The required output photons can be obtained by using the polarizing beamsplitter incorporating the attenuation devices, in which the waveguide loss, the core-effective area, and the TiO_2 length will apply

applications. The optimum FSR of 22 nm is obtained. The few advantages of such a proposed system can be claimed as followings: (1) broadband photon source, (2) wide range power availability, (3) random squeezing photon operation, (4) various detection schemes such as electronic, light, and quantum electronic detections can be applied, and (5) wire and wireless (LiFi) link can be employed. Moreover, the proposed system can be applied for LiFi-quantum link, i.e. free-space link, in which the signal security aspect can be performed, while the high transmission capacity is also available. The long-distance link is also available via the cable connection.

Acknowledgements Prof. P. Yupapin would like to give his acknowledgment of the research facilities to Ton Duc Thang University, Vietnam. Prof. Ali would like to give the appreciation for the research financial support and the research facilities and financial support from the Universiti Teknologi Malaysia, Johor Bahru, Malaysia.

Compliance with ethical standards

Conflict of interest The authors declare that they have no conflict of interest.

References

1. Walls DF (1983) Squeezed states of light. Nature 306:141–146
2. Nakagome H, Ushio H, Itoh Y, Kannari F (2011) Cross phase modulation squeezing in optical fibers. Opt Exp 19(2):1051–1056
3. Dutt A, Luke K, Manipatruni S, Gaeta AL, Nussenzveig P, Lipson M (2015) On-chip optical squeezing. Phys Rev Appl 3:044005
4. Silverstone JW, Santaqati R, Bonneau D, Strain MJ, Sorel M, O'Brien JL, Thompson MG (2015) Qubit entanglement between ring-resonator photon pair sources on a silicon chip. Nat Commun 6:7948
5. Ali J, Pornsuwancharoen N, Youplao P, Aziz M, Amiri I, Chaiwong K et al (2018) Coherent light squeezing states within a modified microring system. Results Phys 9:211–214
6. Khunnam W, Ali J, Amiri IS, Suhailin FH, Singh G, Yupapin P, Grattan KTV (2018) Mode-locked self-pumping and squeezing photons model in a nonlinear micro-ring resonator. Opt Quantum Electron 50:343–348
7. Du C, Huang X, Jiang C et al (2016) Tuning carrier lifetime in InGaN/GaN LEDs via strain compensation for high-speed visible light communication. Sci Rep 6:37132
8. Leitao MF, Santos JMM, Guilhabert B (2017) Gb/s visible light communications with colloidal quantum dot color converters. IEEE J Sel Top Quantum Electron 23(5):1900810
9. Punthawanunt S, Aziz MS, Phatharacorn P, Chiangga S, Ali J, Yupapin P (2018) LiFi cross-connection node model using whispering gallery mode of light in a microring resonator. Microsyst Technol 24(12):4833–4838
10. Wengerowsky S, Joshi SK, Steinlechner F, Ursin R (2018) An entanglement-based wavelength-multiplexed quantum communication network. Nature 564:225–228
11. Steinlechner F, Ecker S, Fink M, Liu B, Bavaresco J, Huber M, Scheidl T, Ursin R (2017) Distribution of high-dimensional entanglement via an intra-city free-space link. Nat Commun 8:15971
12. Pornsuwancharoen N, Youplao P, Amiri IS et al (2018) On-chip polariton generation using an embedded nanograting microring circuit. Results Phys 10:913–916
13. Poznanski RR, Cacha LA, Latif AZA et al (2018) Spontaneous potentiallyas formative cause of thermo-quantum consciousness. J Integr Neurosci 14(4):371–385
14. Dai D, Bowers JE (2014) Silicon-based on-chip multiplexing technologies and devices for Peta-bit optical interconnects. Nanophotonics 3(4–5):283–311
15. Phatharaworamet T, Teeka C, Jomtarak R, Mitatha S, Yupapin PP (2010) Random binary code generation using dark-bright soliton conversion control within a panda ring resonator. IEEE Lightwave Technol 28(19):2804–2809
16. Atabaki AH, Moazenni S, Pavanello S et al (2018) Integrating photonics with silicon nanoelectronics for next generation of system on a chip. Nature 556:349–354
17. Koos C, Jacome L, Poulton C et al (2007) Nonlinear silicon-on-insulator waveguides for all-optical signal processing. Opt Express 15:5976–5990

18. Tan CZ (1998) Determination of refractive index of silica glass for infrared wavelengths by IR spectroscopy. J Non Cryst Solids 223:158–163
19. Banus MD, Reed TB, Strauss AJ (1972) Electrical and magnetic properties of TiO and VO. Phys Rev B 5:2775
20. Pornsuwancharoen N, Amiri IS, Suhailin FH, Aziz MS, Ali J, Singh G, Yupapin P (2017) Micro-current source generated by a WGM of light within a stacked silicon–graphene–Au waveguide. IEEE Photon Technol Lett 29(21):1768–1771